Journal of Magnetic Resonance 277 (2017) 154–161 http://dx.doi.org/10.1016/j.jmr.2017.02.018

"Click" analytics for "click" chemistry – a simple method for calibration-free evaluation of online NMR spectra

Aleksandra Michalik-Onichimowska[*abd], *Simon Kern*[*a],
Jens Riedel[a▪], *Ulrich Panne*[acd], *Rudibert King*[e], *Michael Maiwald*[a]
(* *shared first authorship*)

[a]Bundesanstalt für Materialforschung und -prüfung (BAM), Richard-Willstaetter-Str. 11, D-12489 Berlin, Germany

[b]Physical Chemistry, University of Potsdam, Karl-Liebknecht-Str. 24-25, 14476 Potsdam, Germany

[c]Institut für Chemie, Humboldt-Universität zu Berlin, Brook-Taylor-Str. 2, 12489 Berlin, Germany

[d]School of Analytical Sciences Adlershof, Humboldt-Universität zu Berlin, Zum Großen Windkanal 6, 12489 Berlin, Germany

[e]Department Measurement and Control, Institute of Process Engineering, Berlin University of Technology, Hardenbergstr. 36a, 10623, Berlin, Germany

▪Corresponding author:

Michael Maiwald
Email: Michael.maiwald@bam.de
Phone: +49 30 8104-1140
Bundesanstalt für Materialforschung und -prüfung (BAM), Richard-Willstaetter-Str. 11, D-12489 Berlin, Germany

Abstract

Driven mostly by the search for chemical syntheses under biocompatible conditions, so called "click" chemistry rapidly became a growing field of research. The resulting simple one-pot reactions are so far only scarcely accompanied by an adequate optimization *via* comparably straightforward and robust analysis techniques possessing short set-up times. Here, we report on a fast and reliable calibration-free online NMR monitoring approach for technical mixtures. It combines a versatile fluidic system, continuous-flow measurement of ^{1}H spectra with a time interval of 20 s per spectrum, and a robust, fully automated algorithm to interpret the obtained data. As a proof-of-concept, the thiol-ene coupling between N-boc cysteine methyl ester and allyl alcohol was conducted in a variety of non-deuterated solvents while its time-resolved behaviour was characterised with step tracer experiments. Overlapping signals in online spectra during thiol-ene coupling could be deconvoluted with a spectral model using indirect hard modelling and were subsequently converted to either molar ratios (using a calibration-free approach) or absolute concentrations (using 1-point calibration). For

various solvents the kinetic constant *k* for pseudo-first order reaction was estimated to be 3.9 s^{-1} at 25 °C. The obtained results were compared with direct integration of non-overlapping signals and showed good agreement with the implemented mass balance.

Keywords: NMR spectroscopy, reaction monitoring, automated data evaluation, thiol-ene click chemistry

1. Introduction

Currently research in chemical manufacturing moves towards flexible plug-and-play approaches focusing on modular plants, capable of producing small scales on-demand with short down-times between individual campaigns. This approach allows for efficient use of hardware, a faster optimization of the process conditions and, thus, an accelerated introduction of new products to the market [1]. These systems benefit from integrated processing and control, which translates to increased safety and improved product quality, when appropriate techniques for real-time analytics are applied. This maximization of efficiency of chemical processes efforts goes hand in hand with a synergetic reduction of the negative impact of chemical analyses on the environment and to enable implementation of sustainable development principles to analytical laboratories [2]. Principles for green analytical chemistry comprise among others *in situ* measurements, automated and miniaturized methods as well as multi-analyte methods. All these approaches share the concept of minimizing the sample volume needed for a reliable interrogation.

Techniques employing optical properties of molecules, *e.g.* Raman spectroscopy, IR spectroscopy, UV-VIS spectroscopy, are most commonly applied since they work fast and non-destructive. Albeit they can be integrated inline into the process stream, their real-life applicability is often hampered by problems connected to baseline shift, high background signals and the need for matrix matched standards for calibration.

An alternative to the conventional optical techniques is quantitative NMR spectroscopy applied in flow through mode, which recently matured to a reliable technique for online monitoring and process control [3-5]. NMR spectroscopy can provide structural and quantitative information directly inside complex reacting multicomponent systems. It is

able to obtain information in technical processes, where aromatic-to-aliphatic conversions or isomerizations occur and conventional methods fail due to only minor changes in functional groups.

On behalf of its strict linearity between the number of NMR active nuclei and the detected peak area, which is independent of the matrix, online one-dimensional NMR methods show great potential to obtain quantitative information without time-consuming calibration effort. Ideally, direct integration is the method of choice to extract peak information from spectra when well resolved peaks acquired with stable baseline. Quantitative information can be obtained from ratio of peak area resulting in relative molar ratios or by the use of a concentration conversion factor for the calculation of absolute molar concentrations [6]. Even in the case of partially overlapping signals least squares fitting algorithm and global spectrum deconvolution could successfully be applied for retrieving the individual peak integrals as occurring in an baseline-resolved unperturbed spectrum [7]. Additionally, when it comes to limited resolution leading to strong peak overlaps, ultrafast two-dimensional NMR approaches for reaction monitoring have been successfully demonstrated in literature [8, 9].

Besides problems introduced by signal overlapping in industrial applications of NMR instruments, the automated evaluation of online NMR spectra is often challenged by non-linear effects such as spectral shifts and changes in line shapes. The latter are caused by magnetic field inhomogeneities, or large variations in temperature, pH and pressure. Successful online NMR approaches additionally require to overcome problems related to low signal intensity. The resulting long signal acquisition times become especially critical for monitoring of fast reactions occurring on a timescale of minutes [10].

Linear multivariate methods like partial least square regression (PLS-R) are widely used in industrial applications – often combined with binning in order to compensate variations in the spectra [11-13]. PLS-R performs a data reduction for functionally correlated data by finding factors in the NMR spectra which are also relevant for the quantitative information of the spectra. This is realized by determining a set of latent variables with the constraint that these components explain as much as possible of the covariance between the NMR spectra and the quantitative information. PLS-R models

can be used for many variables but represent major obstacles in model extrapolation and require a high calibration effort.

For the consideration of non-linear effects and fully overlapping signals, spectral modeling based on so-called Indirect Hard Modelling (IHM) shows great potential [14, 15]. This forward convoluting spectral analysis method uses parametrized peak functions to produce flexible spectral models of each component, which appear during reaction monitoring (pure component models). Thereby, the spectrum of a chemical mixture can be composed of the weighted sum of various component models allowing for correction of nonlinear effects. The obtained superposition of peak functions is then iteratively adapted to the recorded spectra *via* least squares algorithms. Subsequently, the weights of these component models in a mixture spectrum can be utilized to construct linear calibration model based on Beer's law. In contrast to most soft modeling methods (e.g. PLS-R) in IHM the physical structure of the spectrum is considered by fixing the peak area ratio in each pure component model during spectral evaluation.

Successful application of IHM to low-field NMR spectra by the use of a linear calibration function has been recently presented in the literature [16, 17]. However, since IHM relies on the fitting with parametrized peak functions, potential for the use of these functions and its area for calibration-free approaches is not fully exploited. To proof its applicability, a reaction scheme providing transformation in a minute/hour timescale was investigated in this study. Thiol-ene coupling offers the above mentioned property and additionally can be highly modified at a small efficiency cost. It is a group of well-established "click" reactions characterized by high conversion rates with reduced degree of by-products formation [18]. Its growing industrial significance for synthetic and material developments impose monitoring when performed on large scale to ensure product quality and optimize the conditions [19-21]. Typical for "click" chemistry, its reaction performance is not restricted to organic solvents and potentially toxic metal-based catalysts. Its feasibility at room temperature in environmentally benign solvents or aqueous solution is only restricted by the solubility behaviour of the applied catalyst. Of special relevance is a fact that reaction may be initiated by photo-catalysis operated at a near visible wavelength (VIS). A number of approaches at different wavelength were proposed to enhance conversion yields and reaction rates

[22]. Still at near-VIS complete reactant transformation may be achieved well below an hour providing optimal conditions for our online NMR spectroscopy test bed.

The Thiol-ene coupling between N-boc cysteine methyl ester and allyl alcohol activated at $\lambda = 365$ nm was chosen as model system. Data achieved by online NMR spectroscopy were processed using direct integration and IHM to show superiority of the latter for fast assessment of compounds concentration without prior calibration.

2. Materials and Methods

2.1. Materials

The chemicals allyl alcohol (≥ 99 %, CAS 107-18-6), N-boc cysteine methyl ester (97 %, CAS 55757-46-5), and 2,2-dimethoxy-2-phenylacetophenone (99 %, CAS 24650-42-8) were supplied by Sigma-Aldrich (Steinheim, Germany) and were used without prior purification.

2.2. Reaction conditions

Thiol-ene coupling was performed between N-boc cysteine methyl ester and allyl alcohol in ratio of 1 to 2.5 molar equivalences, respectively. 0.1 mol of 2,2-dimethoxy-2-phenylacetophenone (DMPA) was added as photoinitiator.

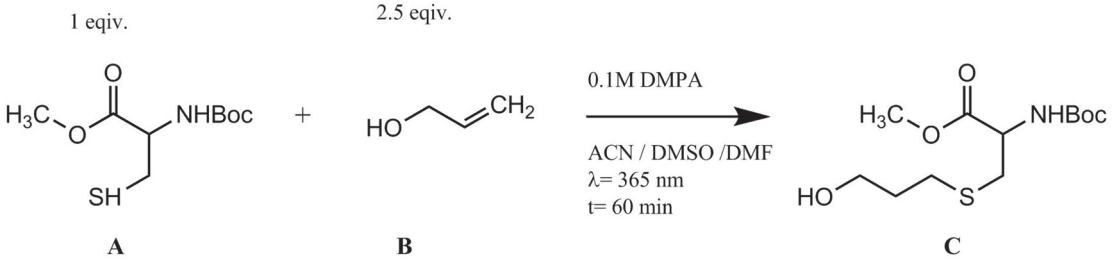

Fig. 1: Reaction mechanism of the thio-ene coupling – A: N-Boc cysteine methyl ester, B: allyl alcohol, C: thioether product

To evaluate the reactions dependence on the surrounding polarity, acetonitrile (ACN), dimethylformamid (DMF), and dimethyl sulfoxide (DMSO) were used as non-deuterated solvents. 0.02 mol of N-Boc cysteine methyl ester and 0.05 mol of allyl alcohol were mixed in a 20 mL measuring flask and filled with a solvent. The

photoinitiator was added to the same respective solvent (2 mmol of DMPA). Prepared reaction mixtures were mixed for 5 minutes and transferred to the batch reactor of 20 mL volume. To maintain constant conditions during reaction monitoring a stirred glass reactor was thermostated at 25 °C. Irradiation was performed for 60 min utilizing a high intensity mercury-xenon lamp (Lightningcure LC8, Hamamatsu Photonics, Hamamatsu City, Japan) with a maximum band intensity at 365 nm. A light guide (quartz glass) was immersed inside the batch reactor to provide uniform irradiation conditions.

2.3. Online monitoring set-up

The experimental set-up for reaction monitoring utilizing 500 MHz NMR spectrometer (Varian Associates, Palo Alto, CA, USA) is presented in Fig. 2. The NMR spectrometer is coupled to a glass reactor (C1) via thermostated PTFE tubing. The circulation of the reaction mixture in between the reactor (C1, 50 mL) and the NMR spectrometer is induced using dosing pump (P1, HPD Multitherm 200, Bischoff Chromatography, Leonberg, Germany). The circulation was split in two loops: i) a fast loop providing flow rate of 6 mL min^{-1} for rapid sample transfer from the reactor to the NMR instrument, and ii) a slow loop of 0.4 mL min^{-1} flow rate resulting in quantitative and pulsation free flow inside the NMR instrument. The latter was obtained by a coriolis massflow controller (FIC, mini Cori-Flow, Bronkhorst High-Tech B.V., Ruurlo, NL) providing accuracy of ± 0.2 % of rate. The reactor as well as the tubing were temperature controlled by a thermostat. In order to prevent solid impurities from entering the tubing system a 15 µm filter (F1) was installed (FISS-FL2-15, FITOK GmbH, Germany) behind the outlet of P1.

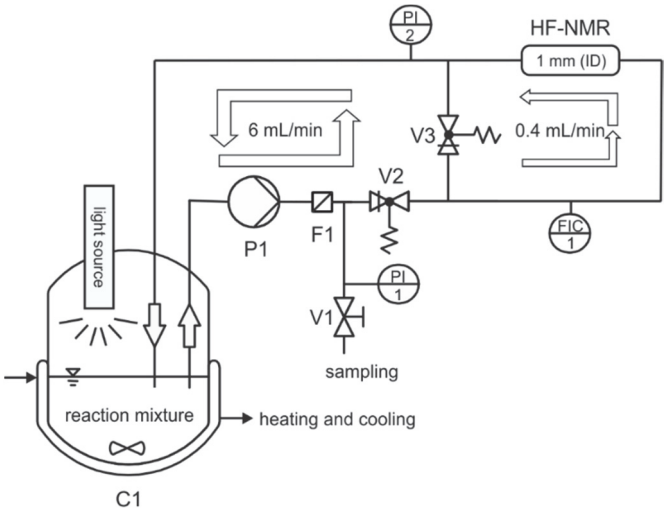

Fig. 2: Flow diagram of the experimental set-up including the by-pass system for online NMR measurements using a 500 MHz NMR spectrometer in continuous flow mode. The bypass stream in between the spectrometer and C1 (50 mL) was split in a fast loop (6 mL/min) and slow loop (0.4 mL/min). The sampling valve V1 was used for additional experiments which are not considered regarding this study.

All spectra were acquired using a 500 MHz spectrometer with a dual band flow probe having a 1/16-inch polymer tubing working as a flow cell. Single scan ^{1}H spectra were recorded with an acquisition time of 5 s, relaxation delay of 15 s and a spectral width of 13.25 ppm.

2.4. Determination of residence time distribution

The flow velocity in the active region of the NMR spectrometer has a great influence on signal intensity when operating in continuous flow mode. The critical flow rates to assure fully magnetized analyte nuclei can be determined by iterative optimization of the normalized signal integral [23]. The resulting comparatively low flow rate providing sample to the NMR in the slow loop (0.5–2 mL min^{-1}) for the flow probe in use and the volume of the tubing system (1.9 mL, 9.5 % of the total applied volume) cause a certain response time of concentration variations in the stirred reactor.

In the interest of characterizing the mixing behavior and residence time distribution (RTD) in detail, a step tracer experiment was conducted by using acetone as tracer. The reactor system, with settings described as in section 2.3, was filled with 20 mL of ACN and 5 mL of acetone was added instantaneously while its propagation in the system was monitored by NMR.

The cumulative distribution $F(t)$ can directly be obtained from the concentration profile of the tracer over time, while the residence time distribution $E(t)$ was calculated by the

numerical gradient of $F(t)$. During step tracer experiment, the tracer solution in the stirred tank gets diluted from fresh solvent returning from the by-pass system to the stirred tank. By this, the resulting curve of $E(t)$ shows the expected oscillation for closed recirculation systems due to re-dilution [24]. For the classification of data into residence time affected and non-affected the following values can be obtained from $F(t)$ as indicated in Fig. 3. The transfer time (t_{trans} = 1.5 min) – the time after which the first amount of tracer cover the distance from the reactor to the active region of the NMR magnet, the delay time (t_{delay} = 3.8 min) – the time after which the tracer concentration has reached its stationary value and the dwell time (t_{dwell} = 2.3 min) – time span between t_{trans} and t_{delay} – have been introduced in the literature [10]. In case of radical formation driven purely by vicinity of light, as shown in the previous section, the reaction occurs mainly in the reactor volume and the reaction mixture flowing through the bypass remains non-irradiated introducing deviations from theoretical behaviour in the observed reaction rate. Still, in the future applications, this effect can be minimized by increasing the reactor volume what was not appropriate for presented herein proof-of-principle studies.

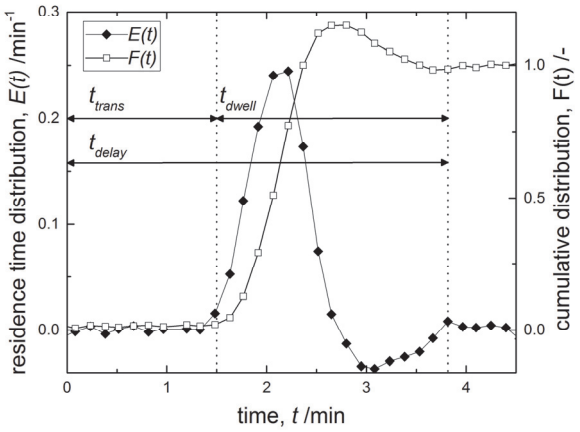

Fig. 3: Cumulative distribution $F(t)$ and residence time distribution function $E(t)$ measured with the NMR instrument in a step tracer experiment, the negative $E(t)$ appears due to re-dilution in the bypass system. The respective times t_{trans}, t_{delay}, t_{dwell} are indicated in the plot.

2.5. Automated data processing of ^{1}H spectra

After acquisition of the FID, the raw data points (32k) were zero-filled to 64k and Fourier transformed in the MATLAB environment. Spectra were corrected by

automated algorithms for baseline and phase adjustments. In order to estimate spectral background, an iterative method fitting a low order polynomial by minimising a non-quadratic cost function was implemented [25]. Optimal zero-order and first-order phase corrections were determined based on entropy minimization [26]. Spectra were aligned to the dominant solvent signals at 1.96, 8.02, and 2.54 ppm for ACN, DMF, and DMSO respectively. Additionally, an exponential line broadening function of 0.1 Hz was applied. A representative proton spectrum before and after processing is shown in the supplementary information.

2.6. Determination of signal areas using IHM and direct integration

In order to analyse the online spectra in respect to their signal areas for each component spectral assignment has to be conducted. Fig. 4 presents the spectral assignment for the reactant mixture as well as for the product mixture after 1 h of reaction time.

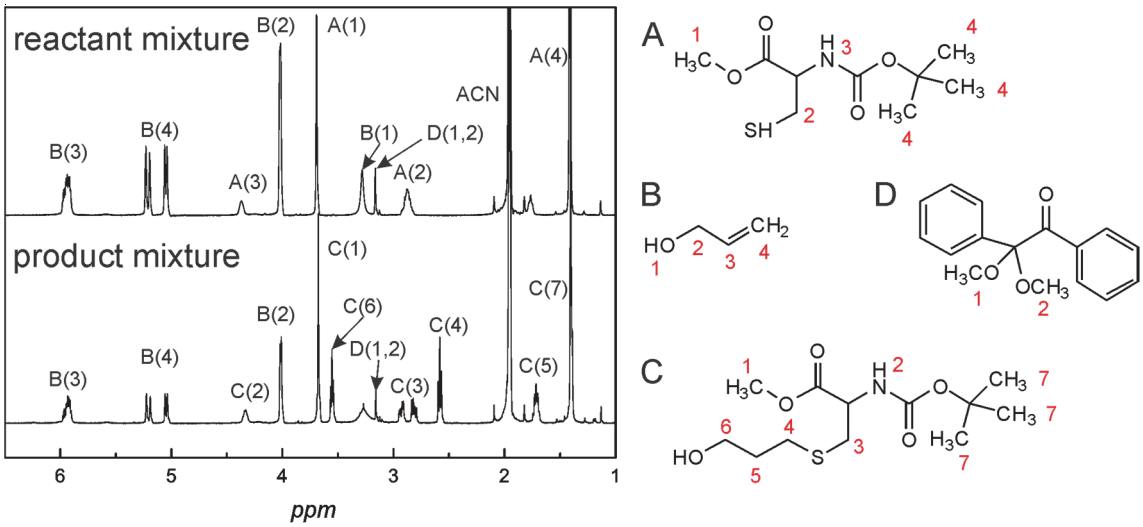

Fig. 4: Spectral assignment of 500 MHz NMR spectra for the reactant mixture and the product mixture after 1 h reaction time. The diastereotopic protons in position 3 of C were summarized to C(3) as well as the vinylic protons in B(4) - A: N-Boc cysteine methyl ester, B: allyl alcohol, C: thioether product, D: 2-phenylacetophenone (DMPA)

IHM was applied to quantitatively resolve overlapping signals A(1) and C(1) of the reactants in reaction mixture spectra by using the software PEAXACT (SPACT GmbH, Aachen, Germany). The overall framework of IHM consists of the succeeding steps. Firstly, a nonlinear spectral model is generated, which is subsequent fitted to the

mixture spectra. Followed conventionally, by a linear calibration model for the prediction of concentrations or ratios from the component fitting results [15].

Regarding the spectral model, pure component models have to be generated by fitting peak functions (Pseudo-Voigt functions) to measured spectra. Based on the spectral assignment, pure component models for N-Boc cysteine methyl ester, allyl alcohol and the thioether product were generated. Therefore, spectra of the final reaction mixture as well as of the initial reaction mixture as shown in Fig. 4 were used. Plots for each pure component model are shown in the supplementary information indicating each single peak function of the models. Additionally, the ranges of interest in the spectra for each component were defined. Solvent signals, OH- and NH- groups of the reactants and the signals of the photoreactant were excluded. Each pure component model consisted of 4 to 14 peak functions with each peak defined by four parameters of the pseudo-Voigt function, the peak maximum α, the width γ, the position δ and the Gaussian-Lorentzian-ratio β (Eq. 1):

$$V = \alpha \left[\beta \exp\left(-4 \ln 2 \frac{(x-\delta)^2}{\gamma^2} \right) + (1-\beta) \frac{\gamma^2}{(x-\delta)^2 + \gamma^2} \right] \qquad \textit{Eq. 1}$$

In Tab. 1, the data range in ppm for each hard model and the respective chemical group are listed. The ranges vary for the respective solvent due to varying overlaps of the solvent signal with the thioether product signal.

Tab. 1: Defined spectral ranges of component models for experiments

hard model	group no.	chem. group	data range /ppm	no. of peaks
N-Boc cysteine methyl ester	A(1)	$-OCH_3$	3.5–3.85	8
Allyl alcohol	B(4)	$=CH_2$	4.85–5.5	4
Product (ACN)	C(1), C(4), C(6)	$-OCH_3$, $-CH_2$, $-CH_2$	3.5–3.85; 2.5–2.7	14
Product (DMSO, DMF)	C(1), C(4), C(5)	$-OCH_3$, $-CH_2$, $-CH_2$	3.5–3.85; 1.65–2.0	14

After generating the component models, a spectral model for mixtures (mixture model) was established. The mixture model consists of a weighted sum of the three reactants (N-Boc cysteine methyl ester, allyl alcohol and the thioether product) component models superimposed with a linear baseline function.

IHM builds each mixture spectrum by fitting weighting factors of each component models to a least squares residual between the mixture model and the measured mixture spectrum (component fitting). During component fitting process, nonlinear effects such as peak line broadening or spectral shifts are taken into account by allowing the variation of peak parameters (Eq. 1) within a constrained range, while the relative peak area in each component model is kept constant. The parameter constraints for the peak position (individual for each peak) and the component shift (shift of all peaks of a component model) showed the most influence on the fitting results. Hereby, the relative boundaries for the peak position was set to 0.05 ppm, the boundaries of component shifts were set to 0.01 ppm while peak maximum and half width was constrained to an relative outer limit of ± 100 %. As fitting mode "very high interaction" was used, which allows the adjustment of all model parameters simultaneously. The result of a component fit for a mixture spectrum is shown in Fig. 5, highlighting the signals A(1), C(1) and C(6).

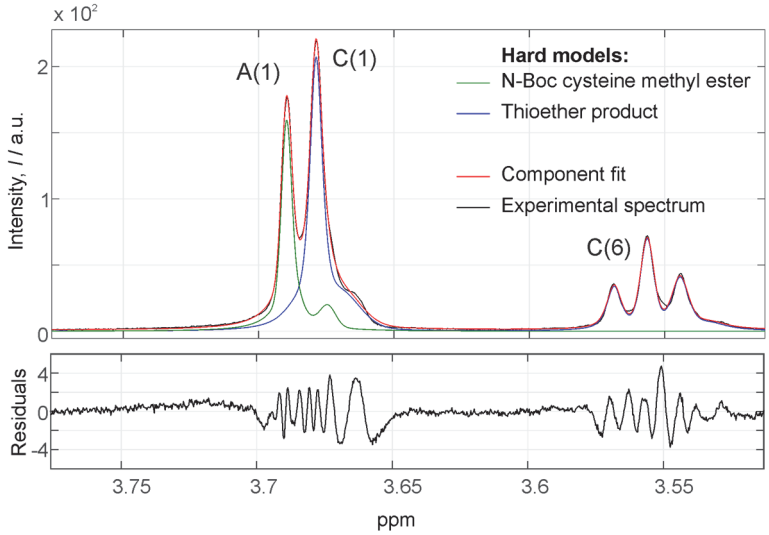

Fig. 5: Representative result for the component fitting of an online NMR spectrum (^{1}H, 500 MHz) after 15 min reaction time during thiol-ene coupling between N-boc cysteine methyl ester and allyl alcohol.

For the direct integration method, the processed NMR spectra were numerically integrated in the intervals provided in Tab. 2 with MATLAB. The acquired signal areas were converted to concentrations and ratios as indicated in section 2.7.

Tab. 2: integration ranges for processed ^{1}H spectra of thiol-ene coupling

reactant	group no.	chem. group	integration range /ppm

Allyl alcohol	B(4)	$=CH_2$	4.95–5.33
Thioether product	C(4)	$-CH_2$	2.5–2.65
Thioether product	C(5)	$-CH_2$	1.65–1.94

2.7. Determination of ratios and concentrations

One of the advantages of NMR spectroscopy as an analytical tool is, that the signal intensity in the spectrum is directly proportional to the number of nuclei responsible for this particular resonance. As a result of this in most cases no need for a linear calibration model is needed, if the signal area and the respective molecular structure which causes the signal are known. Thus, a different approach for IHM was chosen with the benefit of reducing the calibration effort. Instead of a linear calibration model, the concentrations were directly calculated out of the peak areas of the fitted component models.

One of the easiest methods for NMR is the relative quantification method. Hereby, without calibration, the molar ratio x_i can be calculated on the basis of peak area rations by employing the following expression:

$$x_i = \frac{A_i}{\nu_i} \Big/ \sum_{i=0}^{n} \frac{A_i}{\nu_i} \qquad \textit{Eq. 2}$$

where, ν_i is the number of nuclei, A_i is the absolute Integral.

For the absolute quantification method, the use of a concentration conversion factor ξ is needed in order to convert signal areas to molar concentration c_i. ξ was determined via 1-point calibration obtained from the starting concentration of each experiment using Eq. 3:

$$\xi = c_i \cdot \frac{\nu_i}{A_i} \leftrightarrow c_i = \xi \cdot \frac{A_i}{\nu_i} \qquad \textit{Eq. 3}$$

For IHM, the area of each component model was derived from the peak parameters of the Pseudo-Voigt functions with the following equation (cf. Eq. 1):

$$A = \alpha\,\gamma\left[\beta\cdot\sqrt{\pi/\ln 2} + (1-\beta)\cdot\pi\right]$$

Eq. 4

3. Results and discussion

This publication presents an online NMR setup coupled with automated algorithms for spectral processing as well as for the quantification method. To monitor the reaction propagation, IHM was chosen as the favourable evaluation method since it allows resolving the pure peak area of each analyte from the overlapped spectrum measured in the reacting mixture. Through the application of IHM the signal area for each reactant can be deconvoluted from the spectrum and thus converted to the respective molar ratio (calibration-free) or concentration (1-point calibration). However, considering that 1-point calibration method based on a concentration conversion factor (Eq. 3) is non-specific regarding the analyte, the calibration was carried out with the non-overlapping peaks from the starting mixture of the experiments. Linear multivariate methods like PLS-R have not been considered in this application, since these methods require a calibration set throughout the entire concentration range.

The non-overlapping signals, which were suitable for direct integration, were used herein for comparison purposes of both methods.

3.1. Reaction monitoring

Fig. 6 shows concentration time profiles based on the reaction performed in DMSO. The S-H bond is consumed due to the coupling between N-boc cysteine methyl ester and allyl alcohol, whereas their decrease is directly related to the amount of newly produced bond. The presented plot was obtained from single scans proving that applied spectral modelling in combination with highly linear response of the spectrometer provides high quality results allowing for determination of reaction performance. Data points representing an offset from the exponential trend are related to the additional sampling of the reaction mixture performed using valve V1, which induced flow fluctuations in the by-pass system.

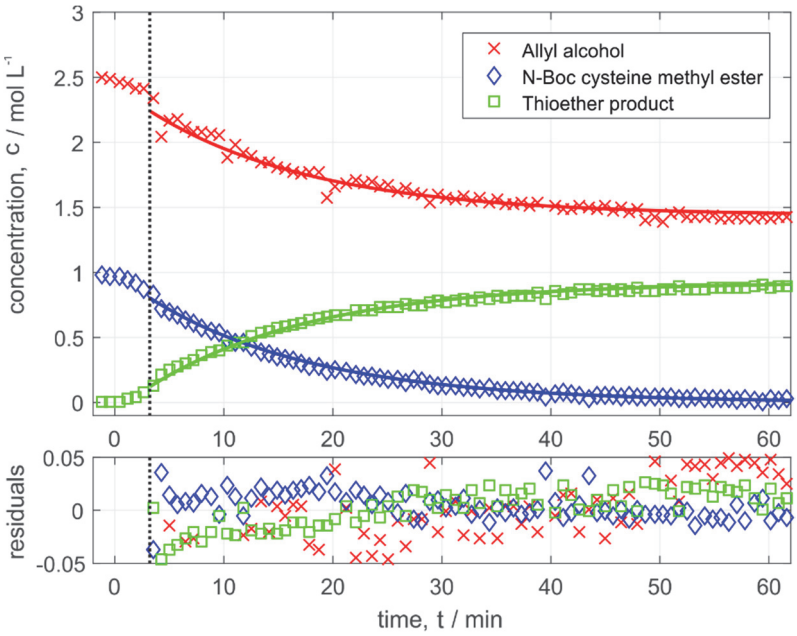

Fig. 6: Comparison of time courses for the photoreaction using DMSO as solvent calculated with IHM (symbols) and fitting results to first order reaction kinetics (lines), residuals of NMR results compared to mass balance of kinetic model. Deviations in Allyl alcohol concentrations were mainly due to withdrawing samples from the reactor.

Moreover, reaction performance was monitored utilizing ACN and DMF as solvent. Fig. 7 provides a comparison of the individual solvents, depicting the respective molar ratio of product over time. These results indicate faster transformation of reactants into thioether product in the initial phase when ACN is used. For DMSO and DMF the rate of product formation in between 5 and 10 min represents a linear increase of 0.013 per min (0.037 mol mL^{-1} min^{-1}), while the reaction performed in ACN shows a slope of 0.02 per min (0.051 mol mL^{-1} min^{-1}). The varying initial reaction rates cause varying turnovers for DMSO, DMF, and ACN after 20 min (72, 71, and 79 %). Nonetheless, for all solvents the limiting reactant (N-boc cysteine methyl ester) was completely consumed after approximately one hour and thus quantitative conversion was achieved. Variations in the final molar ratio of product for the different solvents reach up to 0.05 due to minor deviations in the initial concentration of reactants.

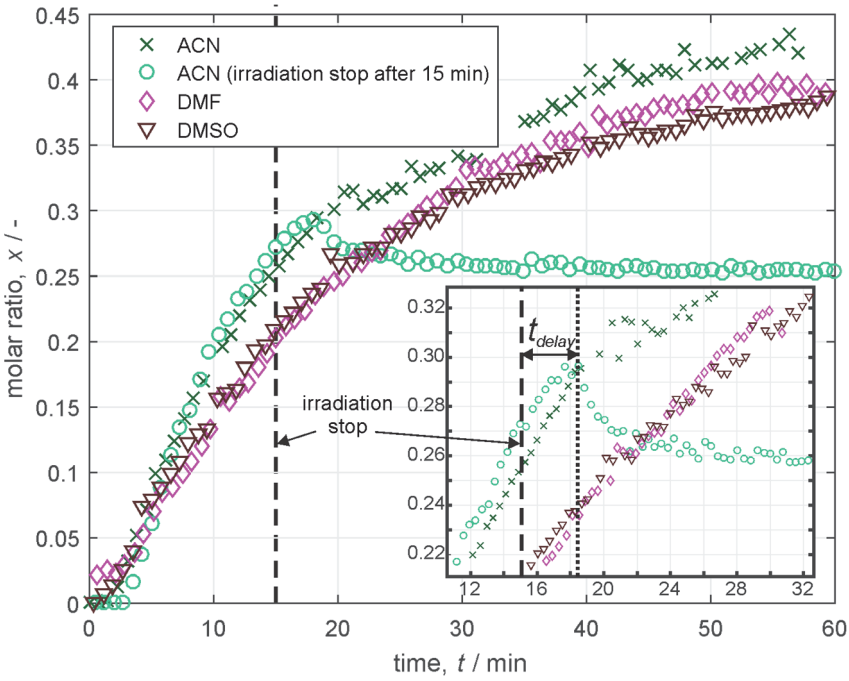

Fig. 7: Time courses of the molar ratio for the thioether product during photoreaction

The described changes in the initial phase of product formation might be subjected to the properties of reaction mixture related to the environment in which transformation occurs. Changes in solvent properties like polarity, viscosity lead to changes in reactant interactions hence reaction rates. Taking into account the solvent polarity index the lowest value is for ACN and the increase for DMF and DMSO being 5.8, 6.4, 7.2, respectively [27]. The same dependence is observed for their density being 0.786, 0.944, and 1.100 g mL^{-1} for ACN, DMF, DMSO respectively. Accordingly, it can be suspected that mixing intensity will vary depending on the solvent and will have the most significant influence in the initial phase of reaction when radicals are produced. The influence of solvent polarity cannot be excluded. However, for the solvents applied throughout this study there is no direct indication of a solvent.

The typical mechanism of the intended radical initiated thiol-ene click chemistry involves two steps: propagation and chain transfer. C-S bond formation is initiated by thiyl radicals created by charge transfer from primarily formed photoinitator radicals. Produced thiyl radicals react with alkenes forming intermediate carbon centered-thioether radical (propagation). The intermediate radical is able to abstract a hydrogen atom, forming the thioether product along with a new thiyl radical (chain transfer),

which can then initiate another propagation step [28]. A detailed scheme of the reaction mechanism is illustrated in the supplementary information.

By terminating the irradiation after 15 minutes reaction propagation by chain transfer step and recombination of light induced radicals was investigated. The exponential results obtained for 15 minutes irradiation is characterized by the same slope as in case of 60 minutes irradiation experiments for the same operating conditions as summarized in *Fig. 7*. Consistency between the results acquired for the first 18 min indicate high reproducibility of the studied chemical system. Investigations of the reaction propagation after the light cut off indicate no significant changes after merely three minutes. The timescale required to detect reaction termination is affected by two mechanisms i) time required for radical recombination ii) the system response being delayed due to the remaining residence time. As described in section 2.4 the delay time to the system is assessed to be 3.8 min nicely coinciding with the detected reaction end-point delay. Hence, radicals formed by the photoinitiation recombine directly (or at least within the temporal resolution of 3 minutes) when the driving force (photons) required for their production is withdrawn. This indicates a negligible contribution of the chain transfer reaction. Line broadening effects, which usually appear when paramagnetic radicals are investigated [29], were not observed, since radicals recombine before they enter the active region of the NMR. The observed product concentration decreases slightly between 21 min and 30 min appears due to the final rinsing of dead volume in the by-pass system and merely reflects fluid dynamic equilibration.

3.2. Material balance and kinetics

According to the above described reaction mechanism reaction kinetics can be differentiated in respect to ratio of propagation and chain transfer rate. Thiols with less abstractable hydrogen atoms, such as alkyl thiols (i.e. N-boc cysteine methyl ester), will tend to have reduced chain transfer rates. This results in rate-limiting chain transfer reactions and thus pseudo-first order reaction kinetics based on thiol concentration [18, 28]. By plotting the logarithm of the experimentally obtained N-boc cysteine methyl ester concentrations over time, a resulting linear behavior justifies this approximation to first order kinetics. In order to validate the quantitative NMR results of IHM a material balance according to Eq. 5 was generated, assuming an irreversible first-order reaction.

$$\frac{\mathrm{d}c_\mathrm{A}}{\mathrm{d}t} = \frac{\mathrm{d}c_\mathrm{B}}{\mathrm{d}t} = -\frac{\mathrm{d}c_\mathrm{C}}{\mathrm{d}t} = -r = kc_\mathrm{A} \qquad \textit{Eq. 5}$$

On the basis of this simple model, the time courses of reactants can be described and fitted to the experimental data. For identification of the model parameters $c_a(t=0)$, $c_b(t=0)$, $c_c(t=0)$, as well as k a simplex search method was used to minimize a objective function, which is based on least squares. By reason of response time in the tubing system the first three minutes of irradiation were neglected during the fitting process. The results of the mass balance of the adapted kinetic model are plotted in Fig. 6. No major trends regarding the residuals were observed, indicating a satisfying quality of the fit. The kinetic constant k (h^{-1}) was estimated to 3.96, 3.92, and 3.94 for experiments using ACN, DMF and DMSO as solvent, respectively. Moreover, the impact of residence time distribution when determining reaction kinetics can be further reduced by modifying the experimental set-up and by introducing $E(t)$ into the mass balance of the kinetic model.

3.3. Uncertainty evaluation

For this study, no reference analytics was available in the interest of validation of NMR results in “traditional” manner. In order to obtain a first estimation of the uncertainty of the presented method, standard deviations of the reactant concentration were calculated for the period of time when concentrations remained constant. An experiment, in which irradiation was terminated after 15 minutes was well suited since concentrations did not change from 45 to 60 min, but all three reactants were still present. Accordingly, absolute standard deviations of 0.011, 0.004 and 0.005 mol L^{-1} were obtained for allyl alcohol, N-boc cysteine methyl ester, and the thioether product, respectively. However, a rigorous in-depth analysis of uncertainty of peak parameters, which were calculated during component fitting, would be beneficial for precise error propagation calculations for peak areas and thus for concentrations. In Fig. 8 the NMR results for IHM and direct integration are compared in a parity plot. While the two methods show a strong coincidence with unity slope (Fig. 8–I) for the allyl concentrations, the obtained thioether product concentrations show a constant offset between direct integration and

IHM (Fig. 8–II). For direct integration the signal C(4) was evaluated, for IHM the signals C(1), C(4) and C(6) were taken into account in the respective pure component model. In general, those signal areas of the same compound show a linear dependency for NMR spectra, although due to failures in baseline correction methods this linearity might stray. This minor overestimation can be compensated by either refining the baseline correction method or by implementing an appropriate calibration model in future work.

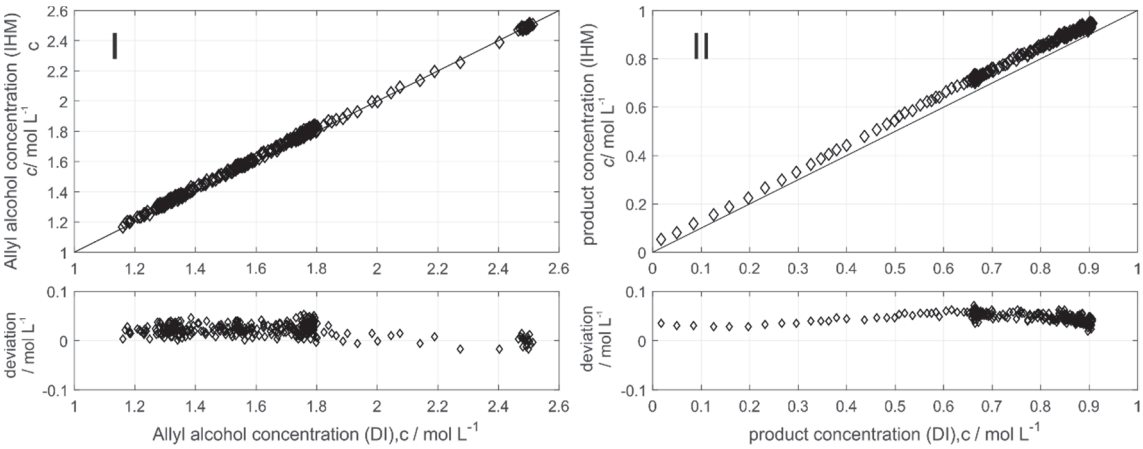

Fig. 8: Direct comparison of reactant concentrations calculated via direct integration (DI) and indirect hard modeling (IHM) for allyl alcohol (*I*) *and the corresponding thioether product* (*II*) *in a parity plot along with deviations c(IHM) – c(DI). The respective considered peaks are listed in Tab. 1 and Tab. 2.*

4. Conclusion

The implemented flow cell NMR set-up for online monitoring in combination with IHM allows quantitative online tracing of reactants during thiol-ene coupling using “click chemistry”. The presented method demonstrates a simple procedure used for evaluation of complex NMR spectra which cannot be evaluated via direct integration. The evaluation method is based on a spectral modeling approach which requires solely pure component spectra and the spectral assignment. This method benefits in comparison to classical PLS-R from quantitative insight in signal areas of pure components in overlapping signals and thus yields a significantly reduced calibration effort and, therefore, exhibits short set-up times. This was shown for adjusting the IHM models for a couple of different solvents in which the reaction was conducted.

The sensitivity of the presented approach allows to identify minor changes in the reaction kinetics when different solvents are applied. Moreover, depicted negligible deviations in concentration during several experiments indicate high repeatability between the measurements. A direct comparison of the two methods, IHM and direct integration, reveal their analogous performance. IHM considers additional peaks, which cannot be resolved utilizing direct integration, providing more flexibility to characterize chemical systems and a more robust analysis. The ultimate advantage of IHM can be anticipated to lie in a quantitative analysis of non-baseline-resolved spectra as they are typical for even more complex reaction mixtures or data obtained on lower field NMR instruments. Thus, the work presented here could eventually pave the road towards a reliable evaluation with low field NMR instruments using permanent magnets in an industrial environment. The extracted data would be beneficial for on-site kinetic studies, screening of novel reactions and optimization of reaction conditions run in small batches.

Acknowledgement

Authors are indebted to Klas Meyer and Nicolai Zientek for help in performing preceding experiments and Andrea Paul for providing the light source. The work of A. Michalik-Onichimowska was financially supported by the Excellence Initiative of the German Research Foundation (DFG). M. Maiwald and S. Kern gratefully acknowledge support from the European Union's Horizon 2020 research and innovation programme under grant agreement N° 636942.

References

[1] A. Adamo, R.L. Beingessner, M. Behnam, J. Chen, T.F. Jamison, K.F. Jensen, J.-C.M. Monbaliu, A.S. Myerson, E.M. Revalor, D.R. Snead, T. Stelzer, N. Weeranoppanant, S.Y. Wong, P. Zhang, On-demand continuous-flow production of pharmaceuticals in a compact, reconfigurable system, Science, 352 (2016) 61-67.
[2] A. Gałuszka, Z. Migaszewski, J. Namieśnik, The 12 principles of green analytical chemistry and the SIGNIFICANCE mnemonic of green analytical practices, TrAC Trends in Analytical Chemistry, 50 (2013) 78-84.
[3] J. Mitchell, L.F. Gladden, T.C. Chandrasekera, E.J. Fordham, Low-field permanent magnets for industrial process and quality control, Progress in Nuclear Magnetic Resonance Spectroscopy, 76 (2014) 1-60.
[4] K. Meyer, S. Kern, N. Zientek, G. Guthausen, M. Maiwald, Process control with compact NMR, TrAC Trends in Analytical Chemistry, DOI http://dx.doi.org/10.1016/j.trac.2016.03.016.
[5] F. Dalitz, M. Cudaj, M. Maiwald, G. Guthausen, Process and reaction monitoring by low-field NMR spectroscopy, Progress in Nuclear Magnetic Resonance Spectroscopy, 60 (2012) 52-70.
[6] S.K. Bharti, R. Roy, Quantitative 1H NMR spectroscopy, TrAC Trends in Analytical Chemistry, 35 (2012) 5-26.
[7] M.A. Bernstein, S. Sýkora, C. Peng, A. Barba, C. Cobas, Optimization and Automation of Quantitative NMR Data Extraction, Analytical Chemistry, 85 (2013) 5778-5786.
[8] M. Gal, M. Mishkovsky, L. Frydman, Real-Time Monitoring of Chemical Transformations by Ultrafast 2D NMR Spectroscopy, Journal of the American Chemical Society, 128 (2006) 951-956.
[9] B. Gouilleux, B. Charrier, E. Danieli, J.-N. Dumez, S. Akoka, F.-X. Felpin, M. Rodriguez-Zubiri, P. Giraudeau, Real-time reaction monitoring by ultrafast 2D NMR on a benchtop spectrometer, Analyst, 140 (2015) 7854-7858.
[10] M. Maiwald, H.H. Fischer, Y.-K. Kim, K. Albert, H. Hasse, Quantitative high-resolution on-line NMR spectroscopy in reaction and process monitoring, Journal of Magnetic Resonance, 166 (2004) 135-146.
[11] J.C. Edwards, P.J. Giammatteo, Process NMR Spectroscopy: Technology and On-Line Applications, in: K.A. Bakeev (Ed.) Process Analytical Technology, John Wiley & Sons, Ltd2010, pp. 303-335.
[12] T.M. Alam, M.K. Alam, Chemometric Analysis of NMR Spectroscopy Data: A Review, Annual Reports on NMR Spectroscopy, Academic Press2004, pp. 41-80.
[13] T.M. Alam, M.K. Alam, S.K. McIntyre, D.E. Volk, M. Neerathilingam, B.A. Luxon, Investigation of Chemometric Instrumental Transfer Methods for High-Resolution NMR, Analytical Chemistry, 81 (2009) 4433-4443.
[14] E. Kriesten, D. Mayer, F. Alsmeyer, C.B. Minnich, L. Greiner, W. Marquardt, Identification of unknown pure component spectra by indirect hard modeling, Chemometrics and Intelligent Laboratory Systems, 93 (2008) 108-119.
[15] E. Kriesten, F. Alsmeyer, A. BardoW, W. Marquardt, Fully automated indirect hard modeling of mixture spectra, Chemometrics and Intelligent Laboratory Systems, 91 (2008) 181-193.
[16] N. Zientek, C. Laurain, K. Meyer, A. Paul, D. Engel, G. Guthausen, M. Kraume, M. Maiwald, Automated data evaluation and modelling of simultaneous 19F–1H

medium-resolution NMR spectra for online reaction monitoring, Magnetic Resonance in Chemistry, 54 (2016) 513-520.
[17] N. Zientek, C. Laurain, K. Meyer, M. Kraume, G. Guthausen, M. Maiwald, Simultaneous 19F–1H medium resolution NMR spectroscopy for online reaction monitoring, Journal of Magnetic Resonance, 249 (2014) 53-62.
[18] C.E. Hoyle, C.N. Bowman, Thiol-Ene Click Chemistry, Angewandte Chemie-International Edition, 49 (2010) 1540-1573.
[19] C. Ligeour, L. Dupin, A. Marra, G. Vergoten, A. Meyer, A. Dondoni, E. Souteyrand, J.J. Vasseur, Y. Chevolot, F. Morvan, Synthesis of Galactoclusters by Metal-Free Thiol "Click Chemistry" and Their Binding Affinities for Pseudomonas aeruginosa Lectin LecA, Eur J Org Chem, DOI 10.1002/ejoc.201402902(2014) 7621-7630.
[20] A. Dondoni, A. Marra, Recent applications of thiol-ene coupling as a click process for glycoconjugation, Chem Soc Rev, 41 (2012) 573-586.
[21] M.A. Cole, C.N. Bowman, Evaluation of thiol-ene click chemistry in functionalized polysiloxanes, J Polym Sci Pol Chem, 51 (2013) 1749-1757.
[22] E.L. Tyson, Z.L. Niemeyer, T.P. Yoon, Redox Mediators in Visible Light Photocatalysis: Photocatalytic Radical Thiol-Ene Additions, Journal of Organic Chemistry, 79 (2014) 1427-1436.
[23] F. Dalitz, M. Maiwald, G. Guthausen, Considerations on the design of flow cells in by-pass systems for process analytical applications and its influence on the flow profile using NMR and CFD, Chemical Engineering Science, 75 (2012) 318-326.
[24] A.D. Martin, Interpretation of residence time distribution data, Chemical Engineering Science, 55 (2000) 5907-5917.
[25] V. Mazet, C. Carteret, D. Brie, J. Idier, B. Humbert, Background removal from spectra by designing and minimising a non-quadratic cost function, Chemometrics and Intelligent Laboratory Systems, 76 (2005) 121-133.
[26] L. Chen, Z.Q. Weng, L.Y. Goh, M. Garland, An efficient algorithm for automatic phase correction of NMR spectra based on entropy minimization, Journal of Magnetic Resonance, 158 (2002) 164-168.
[27] L.R. Snyder, Classification off the Solvent Properties of Common Liquids, Journal of Chromatographic Science, 16 (1978) 223-234.
[28] B.H. Northrop, R.N. Coffey, Thiol-Ene Click Chemistry: Computational and Kinetic Analysis of the Influence of Alkene Functionality, Journal of the American Chemical Society, 134 (2012) 13804-13817.
[29] C. Feldmeier, H. Bartling, K. Magerl, R.M. Gschwind, LED-Illuminated NMR Studies of Flavin-Catalyzed Photooxidations Reveal Solvent Control of the Electron-Transfer Mechanism, Angewandte Chemie International Edition, 54 (2015) 1347-1351.

Journal of Magnetic Resonance 277 (2017) 154–161 http://dx.doi.org/10.1016/j.jmr.2017.02.018

Supplementary Information on

"Click" analytics for "click" chemistry – a simple method for calibration--free evaluation of online NMR spectra

Aleksandra Michalik-Onichimowska[*abd], Simon Kern*[*a], Jens Riedel[a]▪, Ulrich Panne[acd], Rudibert King[e], Michael Maiwald[a]*

(* *shared first authorship*)

[a]Bundesanstalt für Materialforschung und -prüfung (BAM), Richard-Willstaetter-Str. 11, D-12489 Berlin, Germany

[b]Physical Chemistry, University of Potsdam, Karl-Liebknecht-Str. 24-25, 14476 Potsdam, Germany

[c]Institut für Chemie, Humboldt-Universität zu Berlin, Brook-Taylor-Str. 2, 12489 Berlin, Germany

[d]School of Analytical Sciences Adlershof, Humboldt-Universität zu Berlin, Zum Großen Windkanal 6, 12489 Berlin, Germany

[e]Department Measurement and Control, Institute of Process Engineering, Berlin University of Technology, Hardenbergstr. 36a, 10623, Berlin, Germany

Supplementary information

1. Supplementary Figures S1–S2

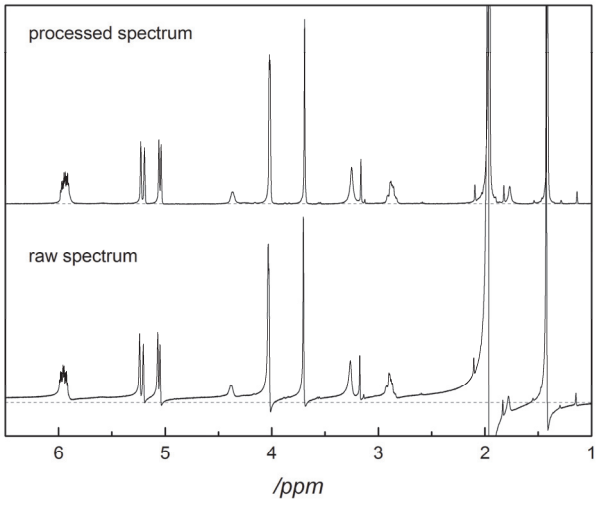

Fig. S1: Representative comparison of 500 MHz NMR spectra during photoreaction using ACN as solvent with automated data processing (assignment see Fig. 5)

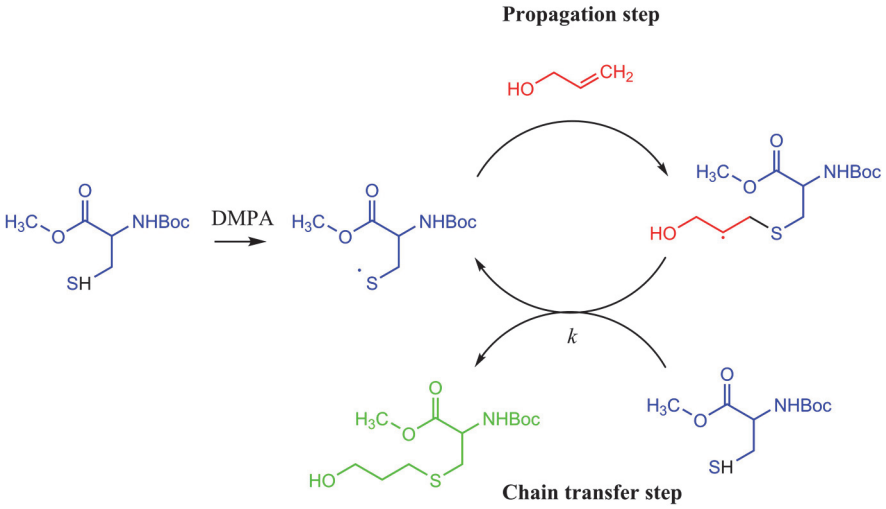

Fig. S2: Mechanism of radical initiated thiol-ene click chemistry for the coupling between N-boc cysteine methyl ester (bue) and allyl alcohol (red). DMPA represents the photoinitator 2,2-dimethoxy-2-phenylacetophenone. (Adapted from Northrop, Brian H., and Roderick N. Coffey. JACS 134.33 (2012): 13804-13817.)

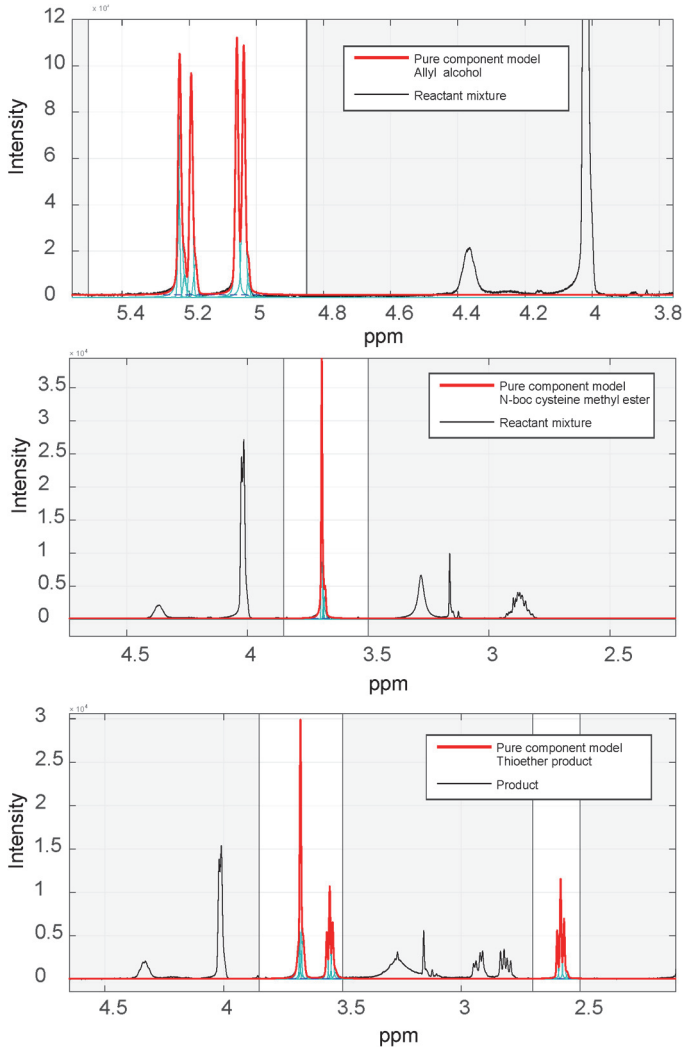

Fig. S3: Pure component models of proton spectra in Acetone for data evaluation using Indirect Hard Modeling